Hysteresis Scaling by Defined Hysteron Pattern in Preisach Model

Teerawat Monnor, Rattikorn Yimnirun, Kanokwan Kanchiang and Yongyut Laosiritaworn

Abstract—**In this work, Preisach model was used to study dynamic hysteresis properties. The patterns of nonlinear relay operators, the hysterons, with sizes of 20×20 hysterons were varied to construct hysteresis loops. The simulation results show that the homogeneous scatter of hysteron results in the symmetric hysteresis loop. On the other hand, the inhomogeneous patterns of the hysteron provide other interesting hysteresis shapes. For instance, with the asymmetric inhomogeneous hysterons, the modeled hysteresis loops are asymmetry, while diagonally symmetric inhomogeneous hysterons yield symmetric hysteresis loops. Then this technique was applied on real hysteresis loops obtained from experiments. The relationship between main characteristic of the hysteresis behavior and hysteron patterns was established. Good agreement between the simulated loops and those from experiments was found indicating the reliability of this Preisach modeling technique in predicting hysteresis behavior for various field perturbations.**

Index Terms—**Hysteresis, hysteron, Preisach model, hysteresis scaling**

I. INTRODUCTION

Hysteresis properties have greatly been concerned in various disciplines. For instance, new methodology in economics predictions [1], sorption hysteresis in wood humidity investigation [2] and observing of saturation magnetization and coercivity for magnetic recording media improvement [3]. Furthermore, hysteresis observation also apparently plays important role in ferroelectric material study, such as ferroelectric thin-film [4-6], nanotube [7] and ceramics [8]. Therefore, as one of the major properties of ferroelectric material, the hysteresis properties have widely been investigated over this field.

Most of the recent works have been accomplished in model of hysteresis loops by means of Preisach model together with neural network technique. For example, artificial neural network was successfully assisted Preisach

Manuscript received June 16, 2012; revised August 16, 2012.

Teerawat Monnor is with the School of Physics, Institute of Science, Suranaree University of Technology, Nakhon Ratchasima 30000, Thailand.

Rattikorn Yimnirun is with the School of Physics, Institute of Science, Suranaree University of Technology, Nakhon Ratchasima 30000, Thailand.

Kanokwan Kanchiang is with the Department of Physics and Materials Science, Faculty of Science, Chiang Mai University, Chiang Mai 50200, Thailand and the Thailand Center of Excellence in Physics, Commission Higher on Education, Ministry of Education, Bangkok 10400, Thailand.

Yongyut Laosiritaworn is with the Department of Physics and Materials Science, Faculty of Science, Chiang Mai University, Chiang Mai 50200, Thailand and the Thailand Center of Excellence in Physics, Commission Higher on Education, Ministry of Education, Bangkok 10400, Thailand (corresponding author to provide phone: +66(0)53943367; fax: +66(0)53943445; e-mail: yongyut_laosiritaworn@yahoo.com).

model to create the hysteresis loops, and then compares with the real measured loop from measurement of magnetic tape [9]. Based on the same implementation, it was satisfied with the good agreement between the modeled and measured hysteresis loop in Fast Tool Servo system [10]. However, the relation between formations of hysteron and simulated hysteresis loops has still been left out. Therefore, to look insight into traditional Preisach model, the patterns of hysteron will be intensively studied to model and to understand lacking behavior in terms of electric phenomena.

This work proposes an efficient technique to simulate the hysteresis loops by means of enhanced Preisach model, which is composed of particularly modified set of nonlinear relay operators. This technique will be introduced in the next part. Then, to achieve the hysteresis loop, the nonlinear relay operator modification will be reviewed. Finally, the results will be showed and discussed.

II. PREISACH MODEL

Preisach model was firstly established in 1935 [11] mainly purposed to model magnetic hysteresis loops. Additionally, it is also successful with hysteresis properties in ferroelectric study. This technique is designed to model the hysteresis loop by driving of nonlinear relay operators called hysterons. Each of them composed of up and down switching as demonstrated in Fig. 1(a) which can be denoted as $R_{\alpha,\beta}$, where $\alpha > \beta$. Fig. 1 shows that, at any occupied state of x, the output y has to be either up or down state. In addition, every hysteron would be defined up/down weight, which is represented the difference between up and down state or it can be referred to increase/decrease of polarization for each hysteron. Based on Preisach model, the weights can be equally or differently defined. This study is modeled in equal weighted hysteron and focused just for hysteron distributed patterns. Then, the set of hysteron can be plotted on the Preisach plane or α,β plane where α has to be greater than β in upper right triangular illustrated in Fig. 1(b).

The hysteresis loops can be approached by linear combination of all weights from all available hysterons associated with the external field varying. In terms of ferroelectric, the polarization at any of external electric field can be approached by Preisach equation in the integration shown in (1) [12,13],

$$P(t) = \int_{-E_m}^{E_m} \int_{-E_m}^{E_m} \rho(\alpha,\beta)\varphi_{\alpha,\beta}[E(t)]d\alpha d\beta \qquad (1)$$

where E_m is a magnitude of dynamic external electric field

($E(t)$), $\rho(\alpha,\beta)$ is Preisach model density function and $\varphi_{\alpha,\beta}[E(t)]$ is the Preisach hysteron operator associated with external field $E(t)$.
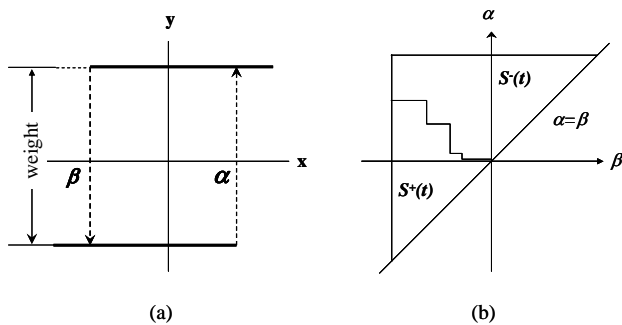

Fig. 1. (a) Up/down switching of hysteron where $\alpha > \beta$ and (b) α,β plane considered specifically for $\alpha > \beta$ area.

In Fig. 1(b), the mentioned right triangular can be geometrically separated into two parts of consideration with the staircase line where $S^+(t)$ is the area of polarization increase or up switching. Conversely, $S^-(t)$ is the fragment of polarization decrease or down switching. Therefore, (1) can be rewritten as

$$P(t) = \iint_{S+} \rho(\alpha,\beta)d\alpha d\beta - \iint_{S-} \rho(\alpha,\beta)d\alpha d\beta \quad (2)$$

In the simulation, the increase and decrease polarization constructed can be examined by summation of all hysteron weights in the following form

$$P(t) = \sum_{i=1}^{m}\sum_{j=1}^{n} \rho(\alpha_i,\beta_j)\varphi_{\alpha_i,\beta_j}[E(t)] \quad (3)$$

where $m \times n$ dimension of hysteron on the plane is evaluated and hysteron weights are included in terms of Preisach density function $\rho(\alpha,\beta)$. Thus, the various hysteron patterns can be constructed the hysteresis loops to study those patterns and their effects to hysteresis properties with strict concerning of equal hysteron weights.

III. HYSTERON PATTERN MODIFICATION

Various hysteron patterns were constructed in this study for both homogeneous and inhomogeneous formation. On one hand, the homogeneous patterns were performed by placing the hysteron with equal interval as the example of 20×20 hysterons illustrated in Fig. 2(a). On the other hand, the hysterons were modified in various arrangements to study the effects of different patterns to the hysteresis properties; loop area, coercivity and remanence. In the latter, the intervals between neighboring hysterons are not equal, and this is called the inhomogeneous pattern in this work. Note that, in both homogeneous and inhomogeneous patterns, the symmetric loops can only be constructed from symmetric pattern, especially diagonal symmetry (i.e. see Fig. 2).

In inhomogeneous formation, various patterns were adjusted based on the highest degree term of polynomial

function, $f(x) = a_n x^n + a_{n-1}x^{n-1} +...+ a_1 x + a_0$, where n is polynomial degree, x is field values (β or α), and $f(x)$ is the Preisach density referring to how dense of the hysteron in field region specified by x . For the examples, a second order polynomial relation i.e. $f(x) = a_2 x^2 + a_0$, was used to generate the arrangements of hysteron as illustrated in Fig. 2(b) and Fig. 2(c). As can be seen, in Fig. 2(b, middle), the hysterons distribution was generated using $f(\beta) = a_{\beta2}\beta^2 + a_{\beta0}$ and $f(\alpha) = a'_{\alpha0}$, which gives high hysteron density at around $\beta = 0$ and its second order polynomial distribution curve is shown above. Note that here $a_{\beta2} < 0$ but $a_{\beta0}, a_{\alpha0} < 0$. On the other hand, in Fig 2(c, middle), the hysterons distribution was generated using

$$f(\beta,\alpha) = a_{\beta2}(\beta + \beta_0)^2 + a_{\alpha2}(\alpha + \alpha_0)^2 + a_0 \quad , \quad \text{where}$$

$\beta_0 = -\alpha_0$, which now gives the distribution pattern with high density around a point diagonally placed on the plane and its 1-D distribution function is shown in Fig. 2(c, top). As a result, based on these systematically defined patterns, the sets of hysteron are ready to be generated hysteresis loop under Preisach model regime. However, in this work, only results obtained from the distribution function as shown in Fig. 2(c) will be emphasized as they provide smooth and symmetric hysteresis shapes.
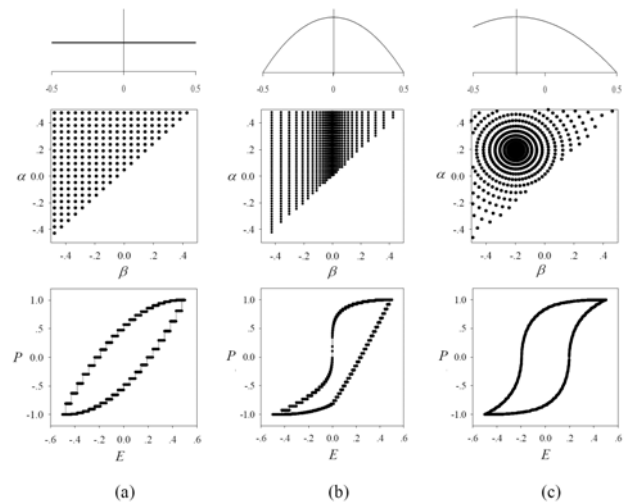

Fig. 2. The distribution curves of hysteron scatter, presenting their illustrated patterns and constructed hysteresis loops for (a) homogeneous 20×20 hysterons, (b) high density of hysteron around $\beta = 0$ and (c) highly distributed hysterons with peak at (-0.2,0.2).

IV. RESULTS AND DISCUSSIONS

Based on Preisach model, hysteron patterns were performed homogenously and inhomogeneously. The homogeneous hysterons construct symmetric loops as an example shown in Fig. 2(a), while the smooth of loop propagations rises with the increase of the number of hysterons. It was found that the number of hysterons affects directly on how smooth of staircase propagation and main shape of the hysteresis loop. However, in the case of inhomogeneous hysterons, there are many interesting features. For instance, after performing Preisach algorithm

with a number of trial hysteron patterns, it is found that the symmetric hysteresis loops are able to be assembled from diagonal symmetric hysteron patterns as examples provided in Fig. 3, where their constructed hysteresis loop shown in below. Conversely, the asymmetric hysteresis can be constructed with various hysteron patterns, as shown in Fig. 2(b). Since consideration of hysteresis loop in asymmetric regimes can be plenty of cases, therefore, the symmetric paradigms are mainly analyzed in this report.
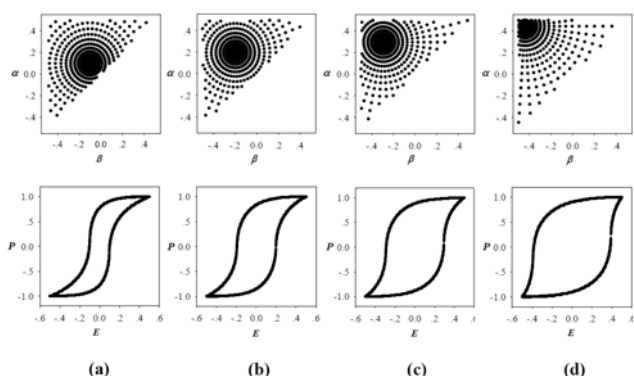

Fig. 3. Inhomogeneous hysterons with high density at points placed diagonally across the diagonal line ($\beta_0 = -\alpha_0$) and their calculated hysteresis loops sequentially shown from nearer to further distance away from the origin.

It was found that the diagonally symmetric patterns of hysteron would be able to construct the symmetric hysteresis loops. In Fig. 3, the radial distances between hysteron rings were characterized by the highest degree term of second order polynomial, yielding high density at a point on considered diagonal line away from the origin of the plane as shown in Fig. 3. The distance between centre of distribution and center of considered plane (0,0) was denoted as R. From the experiment, it can be detailed that the hysteron pattern with larger R creates larger loop area, larger coercivity and larger remanence, as can be investigated in Fig. 3.

To compare the theoretical results with the experimental measurement, the experimental hysteresis loops of BaTiO$_3$ bulk ceramics measured at various frequency of external field were considered as shown in Fig. 4(d). These hysteresis loops were collected at room temperature using Sawyer-Tower circuit with electric field signal (sine wave) generated by HP 3310A generator, where the measurements were performed after reaching the steady state. Details of the experimental setting up can be found elsewhere [14,15]. As can be seen, the relation between theoretical variable R and experimental measurement of loop area, cocercivity and remanence are evident as shown in Fig. 4(a)-(c). It can be seen that the measured loop area (A) and coercivity (C) quite linearly relate to R (see x-labels of Figs. 4(a,b)). However, remanence behaves quite different as non-linear relationship was found (see see x-label of Fig. 4(c)).
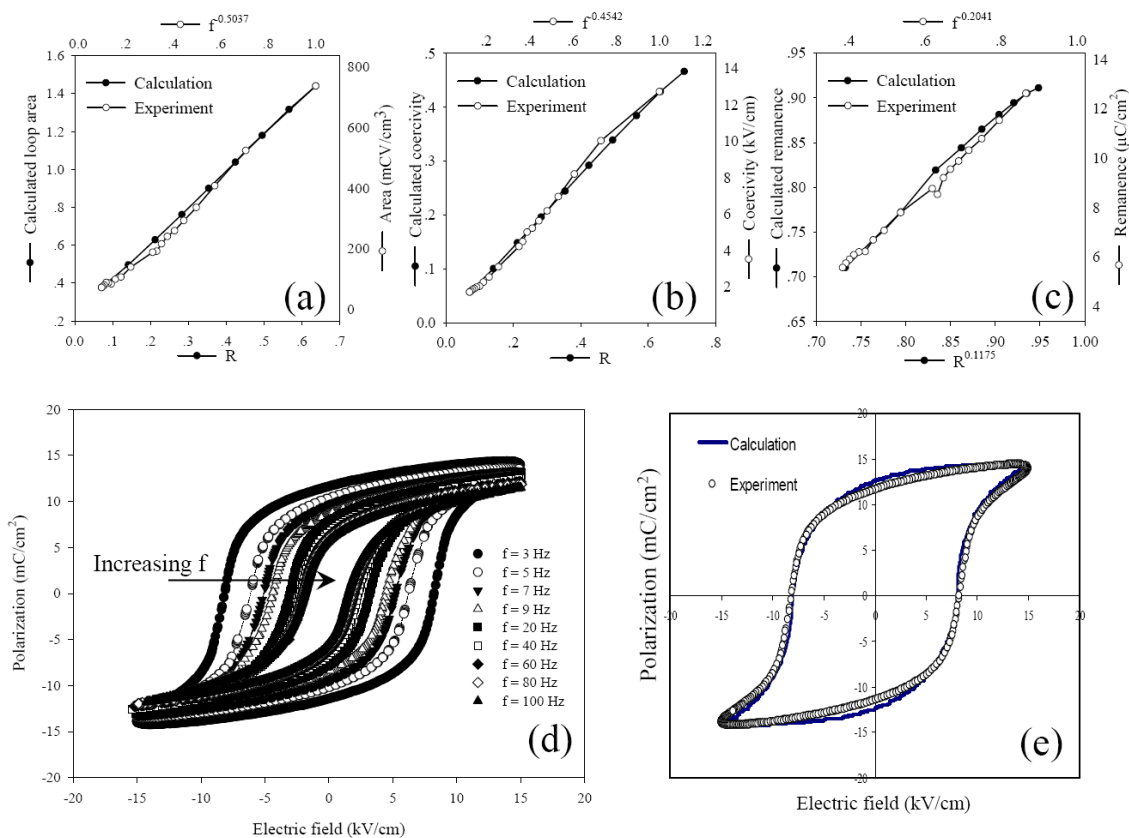

Fig. 4. Hysteresis scaling plots of distance between centre of distribution and distribution peak denoted as R for (a) loop area $A_f = 1192.638R - 20.373$, (b) coercivity $C_f = 19.652R + 0.283$ and (d) remanence $R_f = 35.161R^{0.115} - 20.041$. The measured hysteresis loops with varying frequencies of external field is presented in (d), while (e) presents comparison of a hysteresis loop measured at 3 Hz (filled dots) with that of the recalculated one (solid line).

It is also of interest to calculate empirical formalism that can be used to forecast the R and hysteresis properties relations. Therefore, based on the least-square technique, the scaling relation among R, the constructed hysteresis properties, frequencies of external field and measurable hysteresis properties were established. Specifically, the calculated loop area ($A_f = 1.907R+0.230$), coercivity ($C_f = 0.664R+0.009$) and remanence ($R_f = 0.969R^{0.118}+0.005$) can be scaled with $X_f = af^b + c$, i.e. the relation of measured hysteresis properties (X_f) and frequency of external field (f), where a, b and c are additional constants. With b being equal to -0.504,-0.459 and -0.204 for loop area, coercivity and remanence scaling respectively, the relation of measured hysteresis properties and the calculation parameter R can be obtained as stated in Fig. 4's caption. Further, the averaged R obtained from scaled relation of measured loop area, coercivity and remanence can be used to reconstruct the hysteresis loop. A comparison between the measured loop and the reconstructed loop at a particular field frequency is shown in Fig. 4(e) as an example. The good agreement between recalculated and measured loop can be obviously seen, which affirms the reliability of the Preisach technique used in this study in modeling hysteresis behavior.

V.   CONCLUSION

In this work, it is found that the enhanced Preisach model is a good alternative approach in modeling hysteresis loop. Asymmetric hysteresis loops can be constructed from asymmetry hysteron patterns. On the contrary, the symmetric loop can be constructed by symmetric patterns of hysteron with the diagonal symmetry. Based on the circular distribution of hysteron, the hysteresis properties relate to the hysteron-pattern's radius R, where higher R mostly creates higher loop area, coercivity and remanence. The results are in good agreement with the measured loops for various applied field frequencies.

REFERENCES

[1] R. Cross, "Mach, methodology, hysteresis and economics," J. Phys.: Conf. Ser., vol. 138, pp. 012004, 2008.

[2] S. Merakeb, F. Dubois, and C. Petit, "Modeling of the Sorption Hysteresis for Wood," Wood Sci. Technol. vol. 43, pp. 575–589, 2008.

[3] S. Chiang and Q. Haoxue, "Tuning Magnetic Properties of Magnetic Recording Media Cobalt Ferrite Nano-Particles by Co-Precipitation Method," Symposium on Photonics and Optoelectronics 2009 Proceeding, pp. 1-4, 2009.

[4] V. Shelke, V. N. Harshan, S. Kotru, and A. Guptal, "Effect of kinetic growth parameters on leakage current and ferroelectric behavior of BiFeO3 thin films," J. Appl. Phys., vol. 106, pp. 104114, 2009.

[5] T. H. Lin, C. C. Hsieh, C. W. Luo, J.-Y. Lin, C. P. Sun, H. D. Yang, C.-H. Hsu, Y. H. Chu, K. H. Wu, T. M. Uen, and J. Y. Juang, "Magnetism-induced ferroelectric polarization in the c-axis-oriented orthorhombic HoMnO3 thin films," J. Appl. Phys., vol. 106, pp. 103923, 2009.

[6] F. Gao, G. Wu, H. Zhou, and D. Bao, "Strong upconversion luminescence properties of Yb3+ and Er3+ codoped $Bi_4Ti_3O_{12}$ ferroelectric thin films," J. Appl. Phys., vol. 106, pp. 126104, 2009.

[7] S. S. Nonnenmann, E. M. Gallo, M. T. Coster, G. R. Soja, C. L. Johnson, R. S. Joseph and J. E. Spaniera, "Piezoresponse through a ferroelectric nanotube wall," Appl. Phys. Lett., vol. 95, pp. 232903, 2009.

[8] Z. M. Tian, S. L. Yuan, X. L. Wang, X. F. Zheng, S. Y. Yin, C. H. Wang and L. Liu, "Size effect on magnetic and ferroelectric properties in Bi2Fe4O9 multiferroic ceramics," J. Appl. Phys., vol. 106, pp. 103912, 2009.

[9] A. A. Adly and S. K. Abd–El-Hafiz, "Using neural networks in the identification of Preisach-type hysteresis models," IEEE Trans. Magn., vol. 34, pp. 629-635, 1998.

[10] X. Wang, T. Sun and J. Zhou, "Identification of Preisach Model for a Fast Tool Servo System Using Neural Networks," 2008 IEEE International Symposium on Knowledge Acquisition and Modeling Workshop (KAM 2008 Workshop) Proceeding, 232 (2008).

[11] F. Preisach, "Über die magnetische nachwirkung," Zeitschrift für Physik, vol. 94, pp. 277-302, 1935.

[12] G. Bertotti and M. Pasquale, "Physical interpretation of induction and frequency dependence of power losses in soft magnetic materials," IEEE Trans. Magn., vol. 28, pp. 2787-2789, 1992.

[13] G. Bertotti, "Dynamic generalization of the scalar Preisach model of hysteresis," IEEE Trans. Magn., vol. 28, pp. 2599-2601, 1992.

[14] N. Wongdamnern, J. Tangsritagul, A. Ngamjarurojana, S. Ananta, Y. Laosiritaworn and R. Yimnirun, "Hysteresis scaling relations in polycrystalline $BaTiO_3$ bulk ceramics", Mater. Chem. Phys., vol. 124, pp. 281-286, 2010.

[15] N. Wongdamnern, A. Ngamjarurojana, S. Ananta, Y. Laosiritaworn and R. Yimnirun, "Dynamic hysteresis scaling in $BaTiO_3$ bulk ceramics," Key Eng. Mat., vol. 421-422, pp. 399-402, 2010.